

A Semi-Empirical Formula for Two-Neutrino Double-Beta Decay

O. Nițescu^{1,2,3} and F. Šimkovic^{1,4,*}

¹Faculty of Mathematics, Physics and Informatics,

Comenius University in Bratislava, 842 48 Bratislava, Slovakia

²International Centre for Advanced Training and Research in Physics, P.O. Box MG12, 077125 Măgurele, Romania

³“Horia Hulubei” National Institute of Physics and Nuclear Engineering,
30 Reactorului, POB MG-6, RO-077125 Bucharest-Măgurele, Romania

⁴Institute of Experimental and Applied Physics, Czech Technical University in Prague, 110 00 Prague, Czech Republic

We propose a semi-empirical formula for calculating the nuclear matrix elements for two-neutrino double-beta decay. The proposed model (PM) dependence on the proton and neutron numbers, the pairing, isospin, and deformation properties of the initial and final nuclei is inspired by the insights offered by nuclear many-body methods. Compared with the previous phenomenological and nuclear models, the PM yields the best agreement with the experimental data. Its stability and predictive power are cross-validated, and predictions for nuclear systems of experimental interest are provided.

Introduction.—In 1935, about a year after the Fermi weak interaction theory was introduced [1], Wigner drew attention to the two-neutrino double-beta decay ($2\nu\beta\beta$ -decay):

$$(A, Z) \rightarrow (A, Z + 2) + e^- + e^- + \bar{\nu}_e + \bar{\nu}_e. \quad (1)$$

In this process, two neutrons in the nucleus are converted into two protons while emitting two electrons and two electron antineutrinos. Goepfert-Mayer estimated the half-life of $2\nu\beta\beta$ -decay to be 10^{17} years by assuming a Q -value of about 10 MeV [2]. In 1939, after Majorana formulated the theory of Majorana neutrinos [3], Furry proposed the concept of neutrinoless double-beta decay ($0\nu\beta\beta$ -decay) [4],

$$(A, Z) \rightarrow (A, Z + 2) + e^- + e^-. \quad (2)$$

This process involves two subsequent β decays of neutrons connected via the exchange of virtual neutrinos [5]. There are other modes of double-beta decay transforming the $(A, Z + 2)$ nucleus into the (A, Z) nucleus [6, 7]: the double-positron emitting ($2\nu/0\nu\beta^+\beta^+$) mode, the atomic electron capture with coincident positron emission ($2\nu/0\nu\text{EC}\beta^+$) mode, and the double electron capture ($2\nu/0\nu\text{ECEC}$) mode. These processes are less favored due to smaller Q -value, small overlap of the bound electron wave function with the nucleus, and Coulomb repulsion on positrons.

The primary focus is on studying $0\nu\beta\beta$ -decay, which is not allowed by the Standard Model of particle physics. Thus, it can provide insight into neutrinos' Majorana nature, masses, and CP properties by violating the total lepton number [8–14]. To date, the $0\nu\beta\beta$ -decay has not been observed. The best lower limit on the half-life of this process is approximately $T_{1/2}^{0\nu} \gtrsim 10^{26}$ years for ^{76}Ge [15] and ^{136}Xe [16]. The discovery of $0\nu\beta\beta$ -decay would have far-reaching implications for particle physics and fundamental symmetries.

The first direct observation of $2\nu\beta\beta$ -decay, allowed by the SM, was achieved for ^{82}Se in 1987 [17, 18]. Nowadays, the $2\nu\beta\beta$ -decay has been detected in direct counter

experiments in nine different nuclei, including decays into two excited states. In addition to laboratory experiments, geochemical and radiochemical observations of $2\nu\beta\beta$ -decay transitions have been recorded [19] (and references therein). Furthermore, there are some positive indications of the $2\nu\text{ECEC}$ mode for ^{130}Ba and ^{132}Ba from geochemical measurements [20–22] and for ^{78}Kr [23, 24] and, recently, the first direct observation of the $2\nu\text{ECEC}$ process in ^{124}Xe have been claimed [25, 26]. The measurement of $2\nu\beta\beta$ -decay yields valuable insights into nuclear structure physics, which can be used in $0\nu\beta\beta$ -decay calculations and the search for new physics beyond the SM.

The inverse $2\nu\beta\beta$ -decay half-life is commonly presented as

$$\left(T_{1/2}^{2\nu}\right)^{-1} = |M^{2\nu}|^2 G^{2\nu}, \quad (3)$$

where $G^{2\nu}$ is the phase-space factor (PSF), and

$$M^{2\nu} = g_A^2 M_{GT}^{2\nu} - g_V^2 M_F^{2\nu}, \quad (4)$$

is the nuclear matrix element (NME) governing the transition. g_A and $g_V = 1$ are the axial-vector and vector coupling constants, respectively. The impulse approximation for nucleon current and only $s_{1/2}$ wave states of emitted electrons are considered. The Fermi $M_F^{2\nu}$ and Gamow-Teller (GT) $M_{GT}^{2\nu}$ matrix elements are governed by the Fermi and GT operators, which are generators of isospin SU(2) and spin-isospin SU(4) symmetries, respectively. The isospin is known to be a good approximation in nuclei. Thus, it is assumed that $M_F^{2\nu}$ is negligibly small, and the main contribution is given by $M_{GT}^{2\nu}$, which takes the form

$$M_{GT}^{2\nu} = m_e \sum_n \frac{M_n}{E_n - (E_i + E_f)/2}, \quad (5)$$

with

$$M_n = \langle 0_f^+ \| \sum_m \tau_m^- \sigma_m \| 1_n^+ \rangle \langle 1_n^+ \| \sum_m \tau_m^- \sigma_m \| 0_i^+ \rangle. \quad (6)$$

Here, $|0_i^+\rangle$ ($|0_f^+\rangle$) is the ground state of the initial (final) even-even nuclei with energy E_i (E_f), and the summations run overall $|1_n^+\rangle$ states the intermediate odd-odd nucleus with energies E_n and overall nucleons m inside the nucleus.

The phase-space part of the decay rate can be accurately computed with a relativistic description of the emitted (captured) electrons in a realistic potential of the final (initial) atomic system. The most precise PSFs computed within the self-consistent Dirac-Hartree-Fock-Slater method, including radiative and atomic exchange corrections [27, 28], are presented in Table I. On the other hand, the computation of the NMEs is a challenging and long-standing problem in this field. Due to the growing interest in detecting neutrinoless modes, there have been significant reductions in the uncertainties of half-lives for two-neutrino modes (see $T_{1/2}^{2\nu-\text{exp}}$ form Table I) and consequently of the experimental NMEs, i.e., $M^{2\nu-\text{exp}} = (T_{1/2}^{2\nu-\text{exp}} G^{2\nu})^{-1/2}$ (see Tables II and III). The spread and structure of the experimental NMEs are still poorly understood. A model that aligns with the current experimental NMEs could provide realistic recommendations for future experiments across the nuclear chart.

Currently, the predictions of the $2\nu\beta\beta$ -decay NMEs are based on various nuclear structure models, such as the proton-neutron quasiparticle random phase approximation (pn-QRPA) and its variants [50, 51, 63–74], the nuclear shell model (NSM) [55, 56, 75–81], the interacting boson model (IBM) [52–54, 82], the projected Hartree-Fock-Bogoliubov (PHFB) method [57], effective theory (ET) [58], and others [83, 84], as well as phenomenological models [60–62]. Calculating the $2\nu\beta\beta$ -decay NMEs in nuclear theory is challenging due to the complex structure of open-shell medium and heavy nuclei, and the need to describe a complete set of intermediate nucleus states. Only two approaches have been used for a long time: the pn-QRPA and the NSM. Although limited to low-lying excitations, the NSM accounts for all possible correlations. To match the $2\nu\beta\beta$ -decay data, the Gamow–Teller operator is adjusted (quenched) to fit the results of single β decays or charge exchange reactions, and an unquenched g_A is assumed [56, 75]. The pn-QRPA includes orbitals far from the Fermi surface, considering high-lying excited states (up to 20–30 MeV), but it included fewer correlations. It was found that $M_{GT}^{2\nu}$ and $M_F^{2\nu}$ depend sensitively on the isoscalar and isovector particle-particle interactions of nuclear Hamiltonian, respectively [51, 85]. Recent models like the IBM simplify the low-lying states of the nucleus into $L = 0$ (s boson) or $L = 2$ (d boson) states, focusing on 0^+ and 2^+ neutron pairs converting into two protons. The PHFB formalism obtains nuclear wave functions with good particle number and angular momentum by projecting on axially symmetric intrinsic HFB states. However, it limits the nuclear Hamiltonian

to quadrupole interactions. The impact of this simplification on $M_{GT}^{2\nu}$ calculations is not fully understood. Calculating the $2\nu\beta\beta$ -decay NMEs remains a complex and ongoing task in nuclear theory.

Phenomenological models aim to simplify the process description. For example, according to [86, 87], $2\nu\beta\beta$ -decays with a 1^+ ground state of the intermediate nucleus are determined solely by two virtual β decay transitions. The first connects the initial nucleus with the 1^+ intermediate ground state, and the second connects this 1^+ state with the final ground state. This assumption is the single-state dominance (SSD) hypothesis. One advantage of SSD is its independence from the nuclear structure model, as $M^{2\nu}$ can be determined from measured $\log ft$ values or charge-changing reactions. However, a recent study on electron energy distributions in $2\nu\beta\beta$ -decay of ^{100}Mo [36] suggests that transitions through higher-lying states of the intermediate nucleus also play a crucial role, with destructive interference occurring between these contributions to $M^{2\nu}$.

To our knowledge, three other phenomenological models have been proposed for predicting the $2\nu\beta\beta$ -decay half-lives or NMEs. One model [60] is similar to the Geiger-Nuttall law used for α decay. The other two models [61, 62] suggest that half-lives or NMEs depend on parameters such as the Coulomb energy parameter ($\xi \approx ZA^{-1/3}$), the Q -value, and the quadrupole deformation parameter of the initial nucleus. However, it will be shown later that these models could benefit from refinements to better capture the complexity of the problem.

Phenomenological model.—This letter proposes a phenomenological description of the $2\nu\beta\beta$ -decay NMEs, motivated by nuclear theory findings. The proposed model (PM) is

$$M^{2\nu-ph} = \left(\frac{Z_f}{N_f}\right)^\alpha \left(\frac{\Delta_{\text{pn}}}{1 - \beta_{<}/\beta_{>}}\right)^\gamma (T_f)^\sigma, \quad (7)$$

where Z_f , N_f , and T_f are the proton number, neutron number, and the isospin of the final nuclear ground state, respectively. We note that the ground state of the initial (final) even-even nucleus belongs to the isospin multiplet with $T_i = (N - Z)/2$ ($T_f = (N - Z - 2)/2$) and it is the only state of this nucleus belonging to that multiplet for which the isospin projection equals the total isospin. The dependence of $M_{GT}^{2\nu}$ on the value of the isospin was established in the study performed within an exactly solvable model [85]. The Z/N dependence was motivated by observing that the values of $(Z/N)^{50}T^5$, displayed in Figure 1 and Table III, show a spread similar to $M^{2\nu-\text{exp}}$. The six largest peaks correspond to the NMEs for the $2\nu\beta\beta$ -decay of ^{98}Mo , ^{114}Cd , ^{104}Ru , ^{94}Zr , ^{110}Pd , and ^{100}Mo , in this order. While ^{100}Mo has the largest measured NMEs, theoretical predictions [50, 88, 89] suggest that the other cases might have larger NMEs than ^{100}Mo . Unfortunately, these cases have not yet been measured due to their lower Q -values [90]. It

Table I. The decay properties for various $2\nu\beta\beta$ -decays (right arrow) and 2ν ECEC processes (left arrow). T_f represents the total isospin of the final nucleus. Δ_p and Δ_n denote experimental proton and neutron pairing gaps in units of MeV, respectively. $\beta^{Z,Z+2}$ is the deformation parameter deduced from the corresponding B(E2) transition. $G^{2\nu}$ in yr^{-1} is the most precise PSF computed in this work for $2\nu\beta\beta$ cases and taken from [29] (^{78}Kr , ^{106}Cd , ^{130}Ba , and ^{132}Ba) and [30] (^{124}Xe) for the 2ν ECEC cases. $T_{1/2}^{2\nu\text{-ph}}$ and $T_{1/2}^{2\nu\text{-exp}}$ are the half-lives evaluated with the PM and the experimental half-lives with the smallest uncertainties, respectively. The ^{78}Kr data are for double electron capture from K orbital. For ^{128}Te , the experimental half-life is obtained using the ratio $T_{1/2}^{2\nu\text{-exp}}(^{130}\text{Te})/T_{1/2}^{2\nu\text{-exp}}(^{128}\text{Te}) = (3.52 \pm 0.11) \times 10^{-4}$ [31]. The transitions under the "Fitted" label are used as input for the PM, while those under the "Predicted" label are its predictions.

Nuclear transition	T_f	Δ_p^Z	Δ_n^Z	Δ_p^{Z+2}	Δ_n^{Z+2}	β^Z	β^{Z+2}	$G^{2\nu}$	$T_{1/2}^{2\nu\text{-ph}}$	$T_{1/2}^{2\nu\text{-exp}}$
Fitted										
$^{48}_{20}\text{Ca}_{28} \rightarrow ^{48}_{22}\text{Ti}_{26}$	2	2.179	1.688	1.896	1.564	0.107	0.262	1.58×10^{-17}	1.2×10^{20}	$6.4^{+1.3}_{-1.1} \times 10^{19}$ [32]
$^{76}_{32}\text{Ge}_{44} \rightarrow ^{76}_{34}\text{Se}_{42}$	4	1.561	1.535	1.751	1.710	0.188	0.219	5.07×10^{-20}	1.8×10^{21}	$2.022^{+0.042}_{-0.042} \times 10^{21}$ [33]
$^{82}_{34}\text{Se}_{48} \rightarrow ^{82}_{36}\text{Kr}_{46}$	5	1.401	1.544	1.734	1.644	0.194	0.203	1.68×10^{-18}	9.1×10^{19}	$8.69^{+0.10}_{-0.10} \times 10^{19}$ [34]
$^{96}_{40}\text{Zr}_{56} \rightarrow ^{96}_{42}\text{Mo}_{54}$	6	1.539	0.846	1.528	1.034	0.060	0.172	7.24×10^{-18}	3.4×10^{19}	$2.35^{+0.21}_{-0.21} \times 10^{19}$ [35]
$^{100}_{42}\text{Mo}_{58} \rightarrow ^{100}_{44}\text{Ru}_{56}$	6	1.612	1.358	1.548	1.296	0.231	0.215	3.47×10^{-18}	7.2×10^{18}	$7.07^{+0.11}_{-0.07} \times 10^{18}$ [36]
$^{116}_{48}\text{Cd}_{68} \rightarrow ^{116}_{50}\text{Sn}_{66}$	8	1.493	1.377	1.763	1.204	0.135	0.112	2.91×10^{-18}	2.3×10^{19}	$2.63^{+0.11}_{-0.11} \times 10^{19}$ [37]
$^{130}_{52}\text{Te}_{78} \rightarrow ^{130}_{54}\text{Xe}_{76}$	11	1.104	1.180	1.307	1.248	0.118	0.128	1.62×10^{-18}	7.5×10^{20}	$8.76^{+0.17}_{-0.18} \times 10^{20}$ [38, 39]
$^{136}_{54}\text{Xe}_{82} \rightarrow ^{136}_{56}\text{Ba}_{80}$	12	1.009	1.436	1.265	1.031	0.091	0.125	1.52×10^{-18}	2.5×10^{21}	$2.17^{+0.06}_{-0.06} \times 10^{21}$ [40]
$^{150}_{60}\text{Nd}_{90} \rightarrow ^{150}_{62}\text{Sm}_{88}$	13	1.224	1.046	1.444	1.193	0.285	0.193	3.85×10^{-17}	2.5×10^{19}	$9.3^{+0.7}_{-0.6} \times 10^{18}$ [41]
$^{238}_{92}\text{U}_{146} \rightarrow ^{238}_{94}\text{Pu}_{144}$	25	0.813	0.606	0.662	0.589	0.289	0.285	1.65×10^{-19}	9.1×10^{21}	$2.0^{+0.6}_{-0.6} \times 10^{21}$ [42]
Predicted										
$^{110}_{46}\text{Pd}_{64} \rightarrow ^{110}_{48}\text{Cd}_{62}$	7	1.422	1.442	1.479	1.362	0.257	0.172	1.46×10^{-19}	3.1×10^{20}	$> 10^{18}$ [43]
$^{124}_{50}\text{Sn}_{74} \rightarrow ^{124}_{52}\text{Te}_{72}$	10	1.671	1.314	1.248	1.343	0.0952	0.170	6.00×10^{-19}	1.9×10^{21}	–
$^{128}_{52}\text{Te}_{76} \rightarrow ^{128}_{54}\text{Xe}_{74}$	10	1.129	1.280	1.319	1.265	0.135	0.202	3.00×10^{-22}	1.5×10^{24}	$2.49^{+0.09}_{-0.09} \times 10^{24}$
$^{134}_{54}\text{Xe}_{80} \rightarrow ^{134}_{56}\text{Ba}_{78}$	11	1.134	1.029	1.329	1.176	0.115	0.163	2.25×10^{-23}	4.0×10^{25}	$> 2.8 \times 10^{22}$ [44]
Fitted										
$^{78}_{34}\text{Se}_{44} \leftarrow ^{78}_{36}\text{Kr}_{42}$	5	1.442	1.637	1.577	1.691	0.270	0.256	5.20×10^{-22}	1.7×10^{23}	$1.9^{+1.3}_{-0.8} \times 10^{22}$ [45]
$^{124}_{52}\text{Te}_{72} \leftarrow ^{124}_{54}\text{Xe}_{70}$	10	1.249	1.344	1.357	1.339	0.170	0.223	1.83×10^{-20}	2.0×10^{22}	$1.10^{+0.22}_{-0.22} \times 10^{22}$ [46]
Predicted										
$^{106}_{46}\text{Pd}_{60} \leftarrow ^{106}_{48}\text{Cd}_{58}$	7	1.472	1.401	1.460	1.338	0.162	0.168	5.54×10^{-21}	2.1×10^{21}	$> 4.7 \times 10^{20}$ [47]
$^{130}_{54}\text{Xe}_{76} \leftarrow ^{130}_{56}\text{Ba}_{74}$	11	1.308	1.248	1.351	1.298	0.128	0.215	1.57×10^{-20}	6.0×10^{22}	$2.2^{+0.5}_{-0.5} \times 10^{21}$ [48]
$^{132}_{54}\text{Xe}_{78} \leftarrow ^{132}_{56}\text{Ba}_{76}$	12	1.240	1.181	1.390	1.236	0.141	0.185	4.09×10^{-23}	1.0×10^{26}	$> 2.2 \times 10^{21}$ [49]

Table II. The $2\nu\beta\beta$ -decay NMEs obtained with the proposed model (PM), the ones from the SSD hypothesis, and the most recent calculations from various nuclear structure models. The "Fitted" and "Predicted" nuclei (see caption of Table I) are delimited by " χ^2/N " displaying the chi-squared divided by the number of available data for each set.

Nucleus	$M^{2\nu\text{-th}}$									$M^{2\nu\text{-ph}}$		
	pn-QRPA [50]	pn-QRPA [51]	IBM [52]	IBM [53]	IBM [54]	NSM [55]	NSM [56]	PHFB [57]	ET [58]	$M^{2\nu\text{-exp}}$	PM [59]	SSD
^{48}Ca	–	0.016	0.069	0.024	0.045	–	0.039	–	–	0.0314 ± 0.0030	0.022	–
^{76}Ge	–	0.063	0.083	0.018	0.085	–	0.097	–	0.085	0.0987 ± 0.0010	0.105	–
^{82}Se	–	0.058	0.072	0.024	0.063	0.099	0.105	–	0.156	0.0828 ± 0.0005	0.081	–
^{96}Zr	–	0.133	0.058	0.054	0.034	–	–	0.092	–	0.0770 ± 0.0040	0.063	–
^{100}Mo	0.105	0.251	0.197	0.157	0.045	–	–	0.164	0.179	0.2019 ± 0.0016	0.199	0.174
^{116}Cd	0.112	0.049	0.089	0.069	0.031	–	–	–	0.137	0.1142 ± 0.0027	0.120	0.148
^{130}Te	0.057	0.053	0.035	0.010	0.038	0.027	0.036	0.059	0.034	0.0265 ± 0.0003	0.028	–
^{136}Xe	0.036	0.030	0.056	0.022	0.032	0.024	0.021	–	–	0.0174 ± 0.0002	0.016	–
^{150}Nd	–	–	0.077	0.054	0.017	0.069	–	0.048	–	0.0527 ± 0.0019	0.032	0.023
^{238}U	–	–	–	–	0.023	–	–	–	–	0.0550 ± 0.0110	0.026	–
χ^2/N	5170	2100	2845	2828	1773	470	686	3442	4774	–	30	233
^{110}Pd	0.167	–	–	0.022	0.041	–	–	–	0.211	< 2.61	0.147	–
^{124}Sn	0.023	–	–	–	0.034	0.037	–	–	–	–	0.029	–
^{128}Te	0.051	0.063	0.022	0.018	0.044	0.013	0.049	0.058	0.050	0.0366 ± 0.0007	0.047	0.015
^{134}Xe	0.063	–	–	–	–	–	–	–	–	< 1.25	0.033	–

seems $(Z/N)^{50} T^5$ form captures this ordering of NMEs and is a solid base for improvements.

Table III. The $2\nu\beta\beta$ -decay NMEs obtained with previous phenomenological models [60–62] compared with those predicted by: (A) $(Z_f/N_f)^{50}T_f^5$, (B) $(Z_f/N_f)^{46.94}T_f^{4.90}$, (C) $(Z_f/N_f)^{46.94}T_f^{4.90}\Delta_{\text{pn}}^{0.22}$, (D) $(Z_f/N_f)^{48.44}T_f^{4.95}[\Delta_{\text{pn}}/(\beta_{>} - \beta_{<})]^{0.21}$ and (PM) $(Z_f/N_f)^{46.94}T_f^{4.90}[\Delta_{\text{pn}}/(1 - \beta_{<}/\beta_{>})]^{0.22}$. The "Fitted" and "Predicted" nuclei (see caption of Table I) are delimited by " χ^2_ν " displaying the values of reduced chi-squared (number of DOF) for each model. The last column shows the χ^2_ν when a specific nucleus is involved in the LOOCV for PM.

Nucleus	$M^{2\nu-ph}$									LOOCV for PM χ^2_ν (prediction)
	Previous models			Present models					$M^{2\nu-exp}$	
	[60]	[61]	[62]	A	B	C	D	PM		
^{48}Ca	0.030	0.035	0.037	0.008	0.012	0.020	0.023	0.022	0.0314 ± 0.0030	48 (0.022)
^{78}Ge	0.198	0.123	0.410	0.026	0.044	0.068	0.108	0.105	0.0987 ± 0.0010	41 (0.107)
^{82}Se	0.095	0.096	0.163	0.015	0.027	0.040	0.080	0.081	0.0828 ± 0.0005	35 (0.073)
^{96}Zr	0.060	0.063	0.008	0.027	0.049	0.058	0.068	0.063	0.0770 ± 0.0040	48 (0.063)
^{100}Mo	0.073	0.091	0.220	0.045	0.079	0.110	0.197	0.199	0.2019 ± 0.0016	47 (0.183)
^{116}Cd	0.071	0.093	0.121	0.031	0.058	0.081	0.129	0.120	0.1142 ± 0.0027	49 (0.121)
^{130}Te	0.077	0.068	0.032	0.006	0.014	0.016	0.029	0.028	0.0265 ± 0.0003	32 (0.030)
^{136}Xe	0.030	0.055	0.017	0.004	0.010	0.012	0.016	0.016	0.0174 ± 0.0002	40 (0.015)
^{150}Nd	0.030	0.061	0.203	0.009	0.021	0.025	0.027	0.032	0.0527 ± 0.0019	29 (0.031)
^{238}U	0.024	–	0.046	0.005	0.014	0.010	0.020	0.026	0.0550 ± 0.0110	48 (0.026)
χ^2_ν (ν)	5651 (9)	24981 (2)	17632 (7)	5450 (8)	3171 (8)	2017 (7)	67 (7)	43 (7)		
^{110}Pd	0.135	0.160	0.270	0.047	0.084	0.115	0.143	0.147	< 2.61	
^{124}Sn	0.098	–	0.019	0.009	0.018	0.025	0.029	0.029	–	
^{128}Te	0.067	–	0.042	0.014	0.030	0.037	0.045	0.047	0.0366 ± 0.0007	
^{134}Xe	–	–	0.086	0.010	0.022	0.025	0.033	0.033	< 1.25	

Further refinements involve the quantities $\beta_{<} = \min(\beta^Z, \beta^{Z+2})$ and $\beta_{>} = \max(\beta^Z, \beta^{Z+2})$, which are defined using β^Z and β^{Z+2} , the quadrupole deformation parameters of the initial and final nuclei in their ground states, respectively. This dependence on the deformation parameters reflects the observation from pn-QRPA [70, 71], PHFB [91, 92], and NSM [93] calculations that a mismatch in the deformations of initial and final states reduces the NME value for $2\nu\beta\beta$ -decay. Additionally, the pairing parameter Δ_{pn} is a product of experimental pairing gaps [94],

$$\Delta_{\text{pn}} = \Delta_p^Z \Delta_n^Z \Delta_p^{Z+2} \Delta_n^{Z+2}. \quad (8)$$

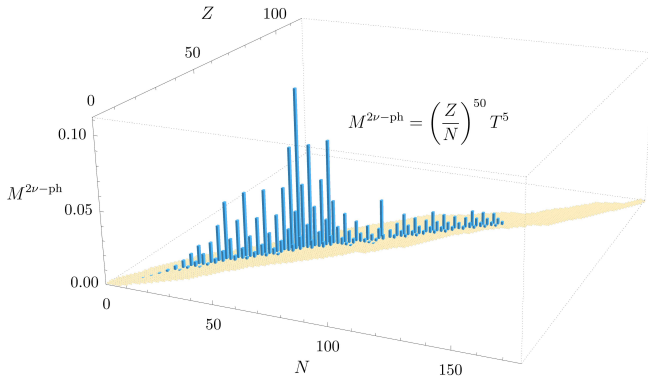


Figure 1. The phenomenological NMEs, obtained using a simplified model $M^{2\nu-ph} = (Z/N)^{50} T^5$, are represented in blue in the (Z, N) space for stable even-even nuclei. The base of the representation, shown in orange, corresponds to the known nuclear chart.

It reflects the significance of transitions through the lowest 1^+ states of the intermediate nucleus. The corresponding β transition amplitudes are linked to the BCS u and v occupation amplitudes, which can be derived from the gap parameter.

The best fitting parameters α , γ , and σ have been obtained from the minimization of the chi-squared

$$\chi^2 = \sum_{i=1}^N \frac{(O_i - P_i)^2}{\sigma_i^2}, \quad (9)$$

where O_i is the experimental NME with uncertainty σ_i , and P_i is the predicted NME. The sum runs over the direct counter experiments and radiochemical observations. The $2\nu\beta\beta$ -decay transitions under the "Fitted" label from Table I ($N = 10$), led to the best PM with $\alpha = 46.94$, $\gamma = 0.22$ and $\sigma = 4.90$. Interestingly, when "Fitted" $2\nu\text{E}CEC$ cases were added as inputs ($N = 12$), but with $T_f \rightarrow T_f + 1$, the same fit parameters were obtained. This might indicate multilevel modeling for both types of transitions, though more half-life measurements for proton-rich nuclei are needed for a clear answer.

Table II compares the $2\nu\beta\beta$ -decay NMEs obtained from the PM, the SSD hypothesis, and the most recent calculations of different nuclear models. These datasets are compared using χ^2/N values. The PM shows the best agreement with experimental NMEs, generally yielding χ^2/N values two orders of magnitude smaller than the other calculations. Note that the values for nuclear models in Table II are the calculated $M_{GT}^{2\nu}$, each multiplied by the square of an effective g_A as chosen by the respective papers. We note smaller χ^2/N values from the SSD hy-

pothesis and NSM calculations, but general conclusions are difficult to draw due to the small number of cases in those datasets. Additionally, we note that the pn-QRPA results from [51], which include a restoration of the SU(4) symmetry and an effective $g_A = 0.904$ based on observed $2\nu\beta\beta$ -decay half-lives, show a considerable decrease in χ^2/N compared to the pn-QRPA study in [50]. In the latter, β -decay observables adjusted the nucleon-nucleon interaction and single-particle energies for each $\beta\beta$ -nuclear system [95].

Table III presents the NMEs from present and previous phenomenological models [60–62] alongside the experimental values. To assess the goodness of fit, we computed the reduced chi-squared $\chi_\nu^2 = \chi^2/\nu$, where ν is the number of degrees of freedom (DOF). We note considerably large χ_ν^2 values for the previous models. The increase in precision has been introduced gradually from the simplified model A to the PM by varying fit parameters and increasing the model’s complexity (see the caption of Table III). The best previous model [60] is similar in precision to the simplified model A. Our study found that considering the deformation overlap is the most critical refinement of the PM.

We applied leave-one-out cross-validation (LOOCV) to assess the robustness of the PM in describing the experimental data and making predictions. LOOCV involves systematically excluding one data point at a time from the fitting procedure and evaluating the performance of the PM on the remaining data. The values of χ_ν^2 for the PM with each exclusion are presented in the last column of Table III. The NME prediction for the excluded case is presented in parentheses. Excluding a specific case scarcely influences the predictions. Moreover, the small variations in χ_ν^2 values confirm the PM’s stability and predictive power.

At first glance, the PM prediction for the $2\nu\beta\beta$ -decay NME for ^{128}Te seems to disagree with the experimental measurement. However, it should be noted that the latter is obtained from the half-lives ratio of ^{130}Te and ^{128}Te , derived from geochemical measurements of ancient tellurium ores [31]. These measurements must be taken with caution, as there might be some unknown production channel of daughter isotopes during their formation. In [96, 97], it is even suggested that obtained results might be affected by a time dependence of the strength of the weak interaction. These possibilities could also influence the measurements of ^{130}Ba and ^{132}Ba . Therefore, we excluded all geochemical cases as inputs from the fit. Only future direct counter experiments on these cases can resolve these ambiguities and confirm the robustness of the PM. Nevertheless, it is interesting to note that the PM predicts quite different NMEs for nuclear systems differing by two neutrons. This is also a feature of the modern nuclear structure models as shown in Table II for ^{130}Te and ^{128}Te . It is also the case of ^{136}Xe and its $2\nu\beta\beta$ partner with two neutrons less, ^{134}Xe . The prediction of

the PM for their NMEs ratio is around 2, and it might be tested in future liquid Xenon experiments [98–101]. Other similar cases are ^{98}Mo , ^{114}Cd , and ^{94}Zr but their very small Q -value limit their near-future measurements.

Conclusions.—In this letter, we proposed a semi-empirical description of the NMEs for two-neutrino double beta decay. Inspired by the findings of nuclear many-body methods, the PM depends on the proton and neutron numbers, pairing, isospin, and deformation properties of the initial and final nuclei. We also found an indication of multilevel modeling for both $2\nu\beta\beta$ -decay and $2\nu\text{ECEC}$ process, but more measurements for proton-rich nuclei are required for a definitive answer. A comprehensive comparison with previous phenomenological and nuclear models revealed that the PM yields the best agreement with the experimental data, explaining the large spread of measured $2\nu\beta\beta$ -decay NMEs. The stability of the PM was confirmed by the LOOCV and reasons to exclude geochemical measurements as inputs were discussed. Finally, we noted that the PM predictions of the NMEs for $2\nu\beta\beta$ nuclear systems differing by two neutrons, are significantly different (by about a factor 2). Its correctness can be checked by measuring additional $2\nu\beta\beta$ transitions.

Acknowledgments.—O.N. acknowledges support from the Romanian Ministry of Research, Innovation, and Digitalization through Project No. PN 23 08 641 04 04/2023. F.Š. acknowledges support from the Slovak Research and Development Agency under Contract No. APVV-22-0413, VEGA Grant Agency of the Slovak Republic under Contract No. 1/0618/24 and by the Czech Science Foundation (GAČR), project No. 24-10180S.

* fedor.simkovic@fmph.uniba.sk

- [1] E. Fermi, *Zeitschrift für Physik* **88**, 161 (1934).
- [2] M. Goeppert-Mayer, *Phys. Rev.* **48**, 512 (1935).
- [3] E. Majorana, *Il Nuovo Cimento* **14** (1937).
- [4] W. H. Furry, *Phys. Rev.* **56**, 1184 (1939).
- [5] G. Racah, *Il Nuovo Cimento* **14** (1937).
- [6] M. Doi and T. Kotani, *Progress of Theoretical Physics* **87**, 1207 (1992).
- [7] M. Doi and T. Kotani, *Progress of Theoretical Physics* **89**, 139 (1993).
- [8] J. Schechter and J. W. F. Valle, *Phys. Rev. D* **25**, 774 (1982).
- [9] Z. Sujkowski and S. Wycech, *Phys. Rev. C* **70**, 052501 (2004).
- [10] S. Pascoli, S. Petcov, and T. Schwetz, *Nuclear Physics B* **734**, 24 (2006).
- [11] S. M. Bilenky and C. Giunti, *International Journal of Modern Physics A* **30**, 1530001 (2015).
- [12] J. D. Vergados, H. Ejiri, and F. Šimkovic, *International Journal of Modern Physics E* **25**, 1630007 (2016).
- [13] I. Girardi, S. Petcov, and A. Titov, *Nuclear Physics B* **911**, 754 (2016).
- [14] F. Šimkovic, *Physics-Uspekhi* **64**, 1238 (2021).

- [15] M. Agostini, G. R. Araujo, A. M. Bakalyarov, M. Balata, I. Barabanov, L. Baudis, C. Bauer, E. Bellotti, S. Belogurov, A. Bettini, *et al.* (GERDA Collaboration), *Phys. Rev. Lett.* **125**, 252502 (2020).
- [16] S. Abe, S. Asami, M. Eizuka, S. Futagi, A. Gando, Y. Gando, T. Gima, A. Goto, T. Hachiya, K. Hata, *et al.* (KamLAND-Zen Collaboration), *Phys. Rev. Lett.* **130**, 051801 (2023).
- [17] S. R. Elliott, A. A. Hahn, and M. K. Moe, *Phys. Rev. Lett.* **59**, 2020 (1987).
- [18] M. K. Moe, *Annual Review of Nuclear and Particle Science* **64**, 247 (2014).
- [19] A. Barabash, *Universe* **6**, 10.3390/universe6100159 (2020).
- [20] A. S. Barabash and R. R. Saakyan, *Physics of Atomic Nuclei* **59**, 179 (1996).
- [21] A. P. Meshik, C. M. Hohenberg, O. V. Pravdivtseva, and Y. S. Kapusta, *Phys. Rev. C* **64**, 035205 (2001).
- [22] M. Pujol, B. Marty, P. Burnard, and P. Philippot, *Geochimica et Cosmochimica Acta* **73**, 6834 (2009).
- [23] Y. M. Gavrilyuk, A. M. Gangapshev, V. V. Kazalov, V. V. Kuzminov, S. I. Panasenko, and S. S. Ratkevich, *Phys. Rev. C* **87**, 035501 (2013).
- [24] S. S. Ratkevich, A. M. Gangapshev, Y. M. Gavrilyuk, F. F. Karpeshin, V. V. Kazalov, V. V. Kuzminov, S. I. Panasenko, M. B. Trzhaskovskaya, and S. P. Yakimenko, *Phys. Rev. C* **96**, 065502 (2017).
- [25] E. Aprile, J. Aalbers, F. Agostini, M. Alfonsi, L. Althueser, F. D. Amaro, *et al.* (XENON Collaboration), *Nature* **568**, 532 (2019).
- [26] E. Aprile, K. Abe, F. Agostini, S. Ahmed Maouloud, M. Alfonsi, L. Althueser, *et al.* (XENON Collaboration), *Phys. Rev. C* **106**, 024328 (2022).
- [27] O. Nițescu, S. Stoica, and F. Šimkovic, *Phys. Rev. C* **107**, 025501 (2023).
- [28] O. Nițescu, R. Dvornický, and F. Šimkovic, *Phys. Rev. C* **109**, 025501 (2024).
- [29] O. Nițescu, S. Ghinescu, S. Stoica, and F. Šimkovic, *Universe* **10**, 10.3390/universe10020098 (2024).
- [30] O. Nițescu, S. Ghinescu, V.-A. Sevostrean, M. Horoi, F. Šimkovic, and S. Stoica, Theoretical analysis and predictions for the double electron capture of ^{124}Xe (2024), [arXiv:2402.13784 \[nucl-th\]](https://arxiv.org/abs/2402.13784).
- [31] T. Bernatowicz, J. Brannon, R. Brazzle, R. Cowsik, C. Hohenberg, and F. Podosek, *Phys. Rev. C* **47**, 806 (1993).
- [32] R. Arnold, C. Augier, A. M. Bakalyarov, J. D. Baker, A. S. Barabash, A. Basharina-Freshville, S. Blondel, S. Blot, M. Bongrand, V. Brudanin, *et al.* (NEMO-3 Collaboration), *Phys. Rev. D* **93**, 112008 (2016).
- [33] M. Agostini, A. Alexander, G. R. Araujo, A. M. Bakalyarov, M. Balata, I. Barabanov, L. Baudis, C. Bauer, S. Belogurov, A. Bettini, *et al.* (GERDA Collaboration), *Phys. Rev. Lett.* **131**, 142501 (2023).
- [34] O. Azzolini, J. W. Beeman, F. Bellini, M. Beretta, M. Biassoni, C. Brofferio, C. Bucci, S. Capelli, V. Caracciolo, L. Cardani, *et al.*, *Phys. Rev. Lett.* **131**, 222501 (2023).
- [35] J. Argyriades, R. Arnold, C. Augier, J. Baker, A. Barabash, A. Basharina-Freshville, M. Bongrand, G. Broudin-Bay, V. Brudanin, A. Caffrey, *et al.*, *Nuclear Physics A* **847**, 168 (2010).
- [36] C. Augier, A. S. Barabash, F. Bellini, G. Benato, M. Beretta, L. Bergé, J. Billard, Y. A. Borovlev, L. Cardani, *et al.* (CUPID-Mo Collaboration), *Phys. Rev. Lett.* **131**, 162501 (2023).
- [37] A. S. Barabash, P. Belli, R. Bernabei, F. Cappella, V. Caracciolo, R. Cerulli, D. M. Chernyak, F. A. Danevich, S. d'Angelo, A. Incicchitti, D. V. Kasperovych, V. V. Kobychyev, S. I. Konovalov, M. Laubenstein, D. V. Poda, O. G. Polischuk, V. N. Shlegel, V. I. Tretyak, V. I. Umatov, and Y. V. Vasiliev, *Phys. Rev. D* **98**, 092007 (2018).
- [38] D. Q. Adams, C. Alduino, K. Alfonso, F. T. Avignone, O. Azzolini, G. Bari, F. Bellini, G. Benato, M. Biassoni, Y. Banaś, *et al.*, *Phys. Rev. Lett.* **126**, 171801 (2021).
- [39] D. Q. Adams, C. Alduino, K. Alfonso, F. T. Avignone, O. Azzolini, G. Bari, F. Bellini, G. Benato, M. Biassoni, A. Branca, *et al.*, *Phys. Rev. Lett.* **131**, 249902 (2023).
- [40] J. B. Albert, M. Auger, D. J. Auty, P. S. Barbeau, E. Beauchamp, D. Beck, V. Belov, C. Benitez-Medina, J. Bonatt, M. Breidenbach, *et al.* (EXO Collaboration), *Phys. Rev. C* **89**, 015502 (2014).
- [41] R. Arnold, C. Augier, J. D. Baker, A. S. Barabash, A. Basharina-Freshville, S. Blondel, S. Blot, M. Bongrand, V. Brudanin, J. Busto, *et al.* (NEMO-3 Collaboration), *Phys. Rev. D* **94**, 072003 (2016).
- [42] A. L. Turkevich, T. E. Economou, and G. A. Cowan, *Phys. Rev. Lett.* **67**, 3211 (1991).
- [43] R. G. Winter, *Phys. Rev.* **85**, 687 (1952).
- [44] X. Yan, Z. Cheng, A. Abdukerim, Z. Bo, W. Chen, X. Chen, C. Cheng, X. Cui, Y. Fan, D. Fang, *et al.* (PandaX Collaboration), *Phys. Rev. Lett.* **132**, 152502 (2024).
- [45] S. S. Ratkevich, A. M. Gangapshev, Y. M. Gavrilyuk, F. F. Karpeshin, V. V. Kazalov, V. V. Kuzminov, S. I. Panasenko, M. B. Trzhaskovskaya, and S. P. Yakimenko, *Phys. Rev. C* **96**, 065502 (2017).
- [46] E. Aprile, K. Abe, F. Agostini, S. Ahmed Maouloud, M. Alfonsi, L. Althueser, B. Andrieu, E. Angelino, J. R. Angevaere, V. C. Antochi, *et al.* (XENON Collaboration), *Phys. Rev. C* **106**, 024328 (2022).
- [47] P. Belli, R. Bernabei, V. Brudanin, F. Cappella, V. Caracciolo, R. Cerulli, F. A. Danevich, A. Incicchitti, D. Kasperovych, V. Klavdiienko, V. Kobychyev, V. Merlo, O. Polischuk, V. Tretyak, and M. Zarytskyy, *Universe* **6**, 10.3390/universe6100182 (2020).
- [48] A. P. Meshik, C. M. Hohenberg, O. V. Pravdivtseva, and Y. S. Kapusta, *Phys. Rev. C* **64**, 035205 (2001).
- [49] A. S. Barabash and R. R. Saakyan, *Physics of Atomic Nuclei* **59**, 179 (1996).
- [50] P. Pirinen and J. Suhonen, *Phys. Rev. C* **91**, 054309 (2015).
- [51] F. Šimkovic, A. Smetana, and P. Vogel, *Phys. Rev. C* **98**, 064325 (2018).
- [52] K. Nomura, Effects of pairing strength on the nuclear structure and double- β decay predictions within the mapped interacting boson model (2024), [arXiv:2406.02986 \[nucl-th\]](https://arxiv.org/abs/2406.02986).
- [53] K. Nomura, *Phys. Rev. C* **105**, 044301 (2022).
- [54] J. Barea, J. Kotila, and F. Iachello, *Phys. Rev. C* **91**, 034304 (2015).
- [55] D. Patel, P. C. Srivastava, V. Kota, and R. Sahu, *Nuclear Physics A* **1042**, 122808 (2024).
- [56] E. Caurier, F. Nowacki, and A. Poves, *Physics Letters B* **711**, 62 (2012).
- [57] P. K. Rath, R. Chandra, K. Chaturvedi, and P. K. Raina, *Frontiers in Physics* **7**, 10.3389/fphy.2019.00064 (2019).

- [58] E. A. Coello Pérez, J. Menéndez, and A. Schwenk, *Phys. Rev. C* **98**, 045501 (2018).
- [59] J. Kotila and F. Iachello, *Phys. Rev. C* **85**, 034316 (2012).
- [60] Y. Ren and Z. Ren, *Phys. Rev. C* **89**, 064603 (2014).
- [61] M. K. P. Rajan, R. K. Biju, and K. P. Santhosh, *Indian Journal of Physics* **92**, 893 (2018).
- [62] B. Pritychenko, *Nuclear Physics A* **1033**, 122628 (2023).
- [63] P. Vogel and M. R. Zirnbauer, *Phys. Rev. Lett.* **57**, 3148 (1986).
- [64] O. Civitarese, A. Faessler, and T. Tomoda, *Physics Letters B* **194**, 11 (1987).
- [65] M. Aunola and J. Suhonen, *Nuclear Physics A* **602**, 133 (1996).
- [66] M. Aunola, O. Civitarese, J. Kauhanen, and J. Suhonen, *Nuclear Physics A* **596**, 187 (1996).
- [67] J. Suhonen and O. Civitarese, *Physics Reports* **300**, 123 (1998).
- [68] S. Stoica and H. Klapdor-Kleingrothaus, *Nuclear Physics A* **694**, 269 (2001).
- [69] S. Stoica and H. Klapdor-Kleingrothaus, *The European Physical Journal A - Hadrons and Nuclei* **17**, 539 (2001).
- [70] F. Šimkovic, L. Pacearescu, and A. Faessler, *Nuclear Physics A* **733**, 321 (2004).
- [71] R. Álvarez-Rodríguez, P. Sarriguren, E. M. de Guerra, L. Pacearescu, A. Faessler, and F. Šimkovic, *Phys. Rev. C* **70**, 064309 (2004).
- [72] V. Rodin, A. Faessler, F. Šimkovic, and P. Vogel, *Nuclear Physics A* **766**, 107 (2006).
- [73] J. Suhonen and O. Civitarese, *Journal of Physics G: Nuclear and Particle Physics* **39**, 085105 (2012).
- [74] F. Šimkovic, V. Rodin, A. Faessler, and P. Vogel, *Phys. Rev. C* **87**, 045501 (2013).
- [75] E. Caurier, F. Nowacki, A. Poves, and J. Retamosa, *Phys. Rev. Lett.* **77**, 1954 (1996).
- [76] E. Caurier, G. Martínez-Pinedo, F. Nowacki, A. Poves, and A. P. Zuker, *Rev. Mod. Phys.* **77**, 427 (2005).
- [77] M. Horoi, S. Stoica, and B. A. Brown, *Phys. Rev. C* **75**, 034303 (2007).
- [78] A. Neacsu and M. Horoi, *Phys. Rev. C* **91**, 024309 (2015).
- [79] B. A. Brown, D. L. Fang, and M. Horoi, *Phys. Rev. C* **92**, 041301 (2015).
- [80] M. Horoi and A. Neacsu, *Phys. Rev. C* **93**, 024308 (2016).
- [81] J. Kostensalo and J. Suhonen, *Physics Letters B* **802**, 135192 (2020).
- [82] J. Barea, J. Kotila, and F. Iachello, *Phys. Rev. C* **87**, 014315 (2013).
- [83] J. Kotila, J. Suhonen, and D. S. Delion, *Journal of Physics G: Nuclear and Particle Physics* **37**, 015101 (2010).
- [84] N. Popara, A. Ravlić, and N. Paar, *Phys. Rev. C* **105**, 064315 (2022).
- [85] D. Štefánik, F. Šimkovic, and A. Faessler, *Phys. Rev. C* **91**, 064311 (2015).
- [86] J. Abad, A. Morales, R. Núñez-Lagos, and A. F. Pacheco, *Il Nuovo Cimento A (1965-1970)* **75**, 173 (1983).
- [87] J. Abad, A. Morales, R. Núñez-Lagos, and A. Pacheco, *Journal de Physique Colloques* **45**, C3 (1984).
- [88] D. A. Nesterenko, L. Jokiniemi, J. Kotila, A. Kankainen, Z. Ge, T. Eronen, S. Rinta-Antila, and J. Suhonen, *The European Physical Journal A* **58**, 44 (2022).
- [89] J. Suhonen, *Nuclear Physics A* **864**, 63 (2011).
- [90] V. I. Tretyak and Y. G. Zdesenko, *Atomic Data and Nuclear Data Tables* **80**, 83 (2002).
- [91] R. Chandra, J. Singh, P. K. Rath, P. K. Raina, and J. G. Hirsch, *The European Physical Journal A - Hadrons and Nuclei* **23**, 223 (2001).
- [92] K. Chaturvedi, R. Chandra, P. K. Rath, P. K. Raina, and J. G. Hirsch, *Phys. Rev. C* **78**, 054302 (2008).
- [93] J. Menéndez, A. Poves, E. Caurier, and F. Nowacki, *Nuclear Physics A* **818**, 139 (2009).
- [94] F. Šimkovic, C. C. Moustakidis, L. Pacearescu, and A. Faessler, *Phys. Rev. C* **68**, 054319 (2003).
- [95] J. T. Suhonen, *Frontiers in Physics* **5**, 10.3389/fphy.2017.00055 (2017).
- [96] P. A. M. Dirac, *Nature* **139**, 323 (1937).
- [97] A. S. Barabash, *Journal of Experimental and Theoretical Physics Letters* **77**, 100 (2003).
- [98] E. Aprile *et al.*, *Journal of Cosmology and Astroparticle Physics* **2017**, 017 (2017).
- [99] D. S. Akerib *et al.* (LUX-ZEPLIN Collaboration), *Phys. Rev. D* **101**, 052002 (2020).
- [100] J. Aalbers *et al.*, *Journal of Cosmology and Astroparticle Physics* **2016**, 016 (2016).
- [101] J. Aalbers *et al.*, *Journal of Physics G: Nuclear and Particle Physics* **43**, 015101 (2016).